Heliyon 9 (2023) e13629

Contents lists available at ScienceDirect

Heliyon

journal homepage: www.cell.com/heliyon

Research article

Effects of KMT2D mutation and its exon 39 mutation on the immune microenvironment and drug sensitivity in colorectal adenocarcinoma

Chuan Liu [a], Yuzhi Jin [a], Hangyu Zhang [a], Junrong Yan [b], Yixuan Guo [a], Xuanwen Bao [a,*], Peng Zhao [a,**]

[a] Department of Medical Oncology, The First Affiliated Hospital, School of Medicine, Zhejiang University, Hangzhou 310003, Zhejiang Province, People's Republic of China

[b] Medical Department, Nanjing Geneseeq Technology Inc., Nanjing 210032, Jiangsu Province, People's Republic of China

ARTICLE INFO

Keywords:
KMT2D
Exon 39
Mutation
Colorectal adenocarcinoma
Immune microenvironment
Drug sensitivity

ABSTRACT

Background: KMT2D mutation (KMT2D^{MT}) was found to play an important role in cancer immunity and response to immune checkpoint inhibitors (ICIs). The present study aims to investigate the association between KMT2D exon 39 mutation (K-ex39^{MT}) and molecular and clinical characteristics in colorectal adenocarcinoma (CRAD).

Methods: We performed profiling of KMT2D^{MT} and K-ex39^{MT} via Kaplan–Meier analysis, cBioportal, Immune-related functional analysis and correlation analysis with TCGA and MSK cohorts to explore their effects on the prognosis, immune landscape, molecular characteristics and drug sensitivity in CRAD. Panel gene sequencing of 30 in-house CRAD tissues and multiple immunofluorescences (mIF) were also used.

Results: In multi-cancer, patients with KMT2D^{MT} have a worse overall survival (OS), and CRAD with K-ex39^{MT} exhibited a greater degree of immune cellular infiltration. For CRAD, compared with KMT2D exon39 wild type (K-ex39^{WT}), K-ex39^{MT} patients had higher tumor mutational burden (TMB) and lower copy number alteration (CNA), and were accompanied by more immune cell infiltration including activated T cells, NK cells, Treg cells and exhausted T cells and enrichment of immune-related genes and pathways. In drug sensitivity prediction, K-ex39^{MT} patients have a lower CTX-S score and IC50 of 5-Fluorouracil and irinotecan, and higher Tumor Immune Dysfunction and Rejection (TIDE) dysfunction score.

Conclusions: CRAD patients with K-ex39^{MT} have more abundant immune cell infiltration and enrichment of immune-related pathways and signatures. And they may be more sensitive to some chemotherapies but less to cetuximab.

1. Introduction

Immunotherapy has gradually become the mainstay of cancer treatment in recent years, with immune checkpoint inhibitors (ICIs) such as programmed cell death protein ligand 1 (PD-L1) antibodies and cytotoxic T lymphocyte-associated antigen 4 (CTLA-4)

* Corresponding author.
** Corresponding author.
E-mail addresses: baoxuanwen@gmail.com (X. Bao), zhaop@zju.edu.cn (P. Zhao).

https://doi.org/10.1016/j.heliyon.2023.e13629
Received 13 September 2022; Received in revised form 2 February 2023; Accepted 6 February 2023
Available online 10 February 2023

antibodies becoming the first-line treatment for a range of advanced cancer patients [1–3]. Although several studies have indicated that ICIs improve survival and treatment tolerance, the medication's limits and long-term benefits vary per patient [4]. Several predictive markers, such as PD-L1 expression [5], high microsatellite instability (MSI-H) [6–8], and tumor mutational burden (TMB) [5] have been steadily validated and employed in the clinic to predict the treatment response of cancer patients to ICIs. Additionally, copy number alteration (CNA) [9] and tumor immune microenvironment (TME) [10] were also discovered to be associated with ICI response. However, there are several restrictions to the use of these markers. In a phase II trial KEYNOTE-158, for example, the majority of MSI-H/deficient mismatch repair (dMMR) patients reacted to pembrolizumab (objective response rate: 34.3%), although a small percentage of patients did not respond to ICI treatments [11]. In another KEYNOTE-042 trial, patients with low PD-L1 expression also benefited from ICIs [12]. As a result, new markers for predicting immunotherapy in cancer patients are needed.

Mutations in genes are a common cause of cancer. It has also been linked to the response to various treatment regimens and has the potential to disrupt the immunological microenvironment. KRAS mutations are found in a wide range of malignancies, and treatment options for people with KRAS mutations, such as chemotherapy and targeted therapy, are ineffective [13]. Early in tumor growth, KRAS mutation-driven cancer cells alter the cellular composition and TME vascularity and structure, as well as induce inflammatory signaling, while interacting with external stimuli to create an inflammatory environment that improves oncogenicity [14]. Furthermore, mutations in gene exons are linked to cancer patient prognosis and have become therapeutic targets. Lung cancer patients with EGFR exon 20 deletion mutations are resistant to targeted therapies and have a poor prognosis [15,16]. Therefore, cancer patients will be affected by both gene and exon alterations.

Mutations in KMT2D are also prevalent in malignancies, including lung cancer [17,18] and prostate cancer [19,20]. KMT2D

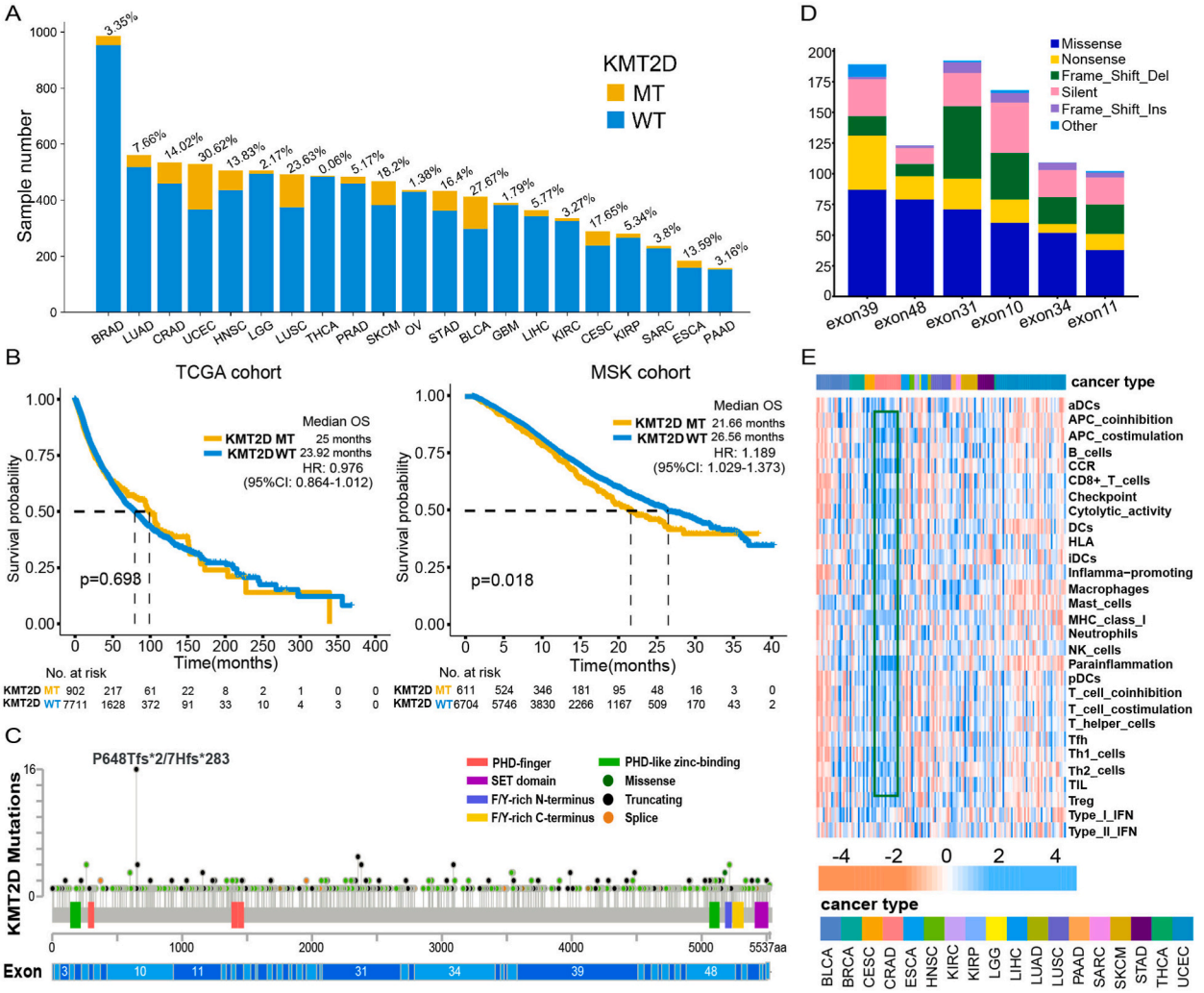

Fig. 1. KMT2D^{MT} and K-ex39^{MT} in pan cancer; **(A)** Proportion of patients with KMT2D^{MT} in 21 malignancies; **(B)** Kaplan-Meier curves of OS in KMT2D^{MT} and KMT2D^{WT}of 21 malignancies in TCGA and MSK-IMPACT cohorts; **(C)** Distribution of KMT2D^{MT} according to KMT2D domains and exons in the TCGA cohort; **(D)** Proportion of mutation types in the top six exons with the highest mutation rate in KMT2D; **(E)** Immune infiltration in K-ex39^{MT} patients of 21 malignancies. KMT2D^{MT}: KMT2D mutation type; K-ex39^{MT}: KMT2D exon 39 mutation type; KMT2D^{WT}: KMT2D wild type.

mutation type (KMT2D^{MT}) has been demonstrated to cause genomic instability and transcriptional stress, both of which promote tumorigenesis reported in the previous investigations [21]. KMT2D^{MT} tumor samples displayed much higher infiltration of antigen-presenting cells and T cells in preclinical experiments, making them more vulnerable to ICIs [22]. Using the TCGA cohort, we first explored the predictive impact of KMT2D^{MT} in 21 solid tumors. The predictive function of KMT2D exon39 mutation type (K-ex39^{MT}) in colorectal adenocarcinoma (CRAD) patients was then investigated in depth. We discovered that CRAD patients with K-ex39^{MT} had a worse prognosis than wild-type patients, but that these mutations were closely linked to improved antitumor immunity and consequently higher chemotherapy and ICI sensitivity.

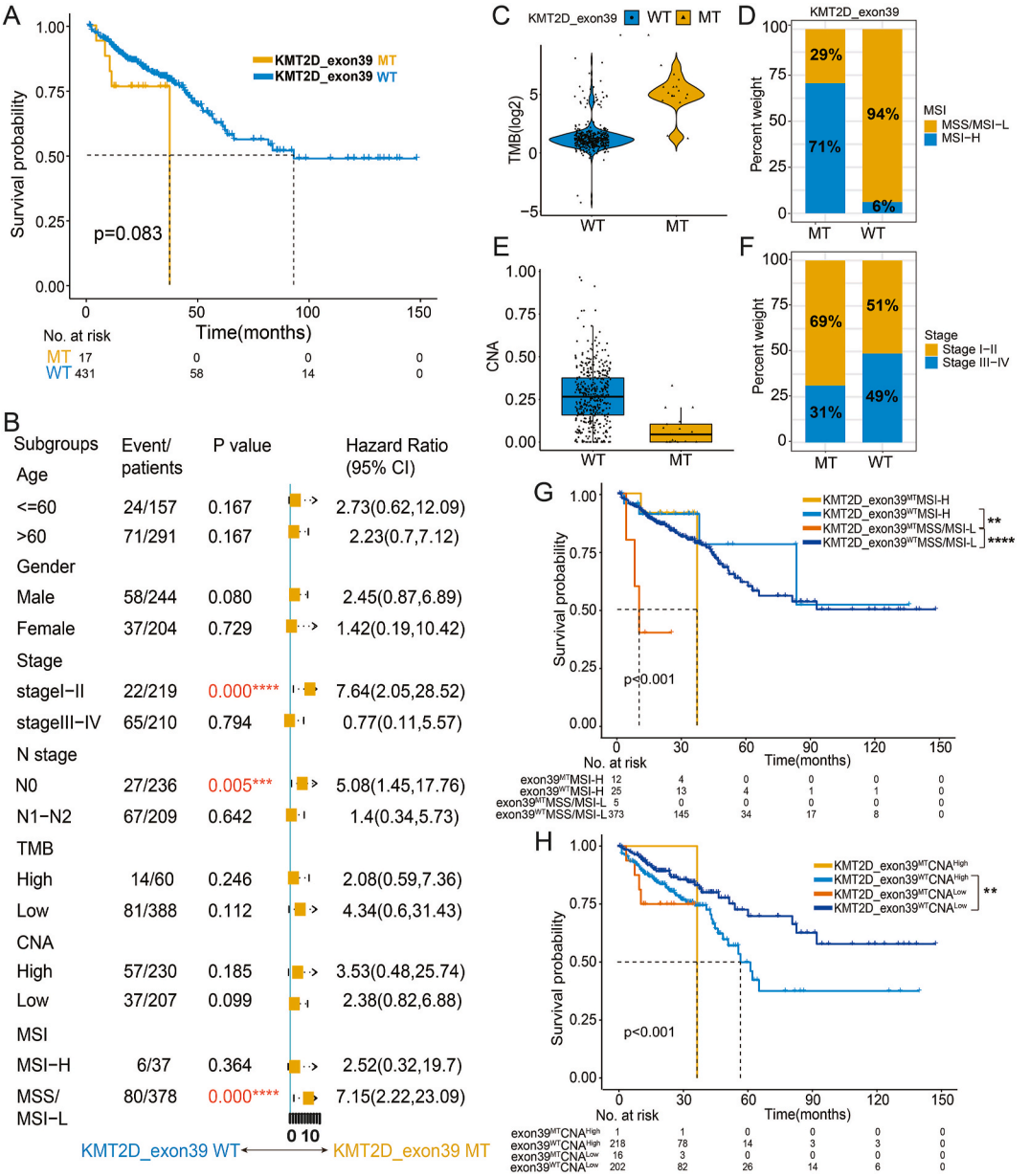

Fig. 2. **(A)** Kaplan-Meier curves of OS in K-ex39^{MT} and K-ex39^{WT} patients of CRAD in the TCGA cohort; **(B)** Forest plot depicting subpopulation analysis in TCGA cohort; **(C–F)** Log2 (TMB), MSI, CNA and AJCC stage in K-ex39^{MT} and K-ex39^{WT} patients; **(G)** The Kaplan-Meier curves of OS among K-ex39^{MT}MSI-H, K-ex39^{MT}MSI-L/MSS, K-ex39^{WT}MSI-H, and K-ex39^{WT}MSI-L/MSS groups in CRAD patients; **(H)** The Kaplan-Meier curves comparing OS among K-ex39^{MT}CNA^{High}, K-ex39^{MT}CNA^{Low}, K-ex39^{WT}CNA^{High}, and K-ex39^{WT}CNA^{Low} groups in CRAD patients. OS: overall survival; K-ex39^{MT}: KMT2D exon 39 mutation type; K-ex39^{WT}: KMT2D exon 39 wild type; TMB: tumor mutation burden; MSI: microsatellite instability; CNA: copy number alteration; MSS: microsatellite stability.

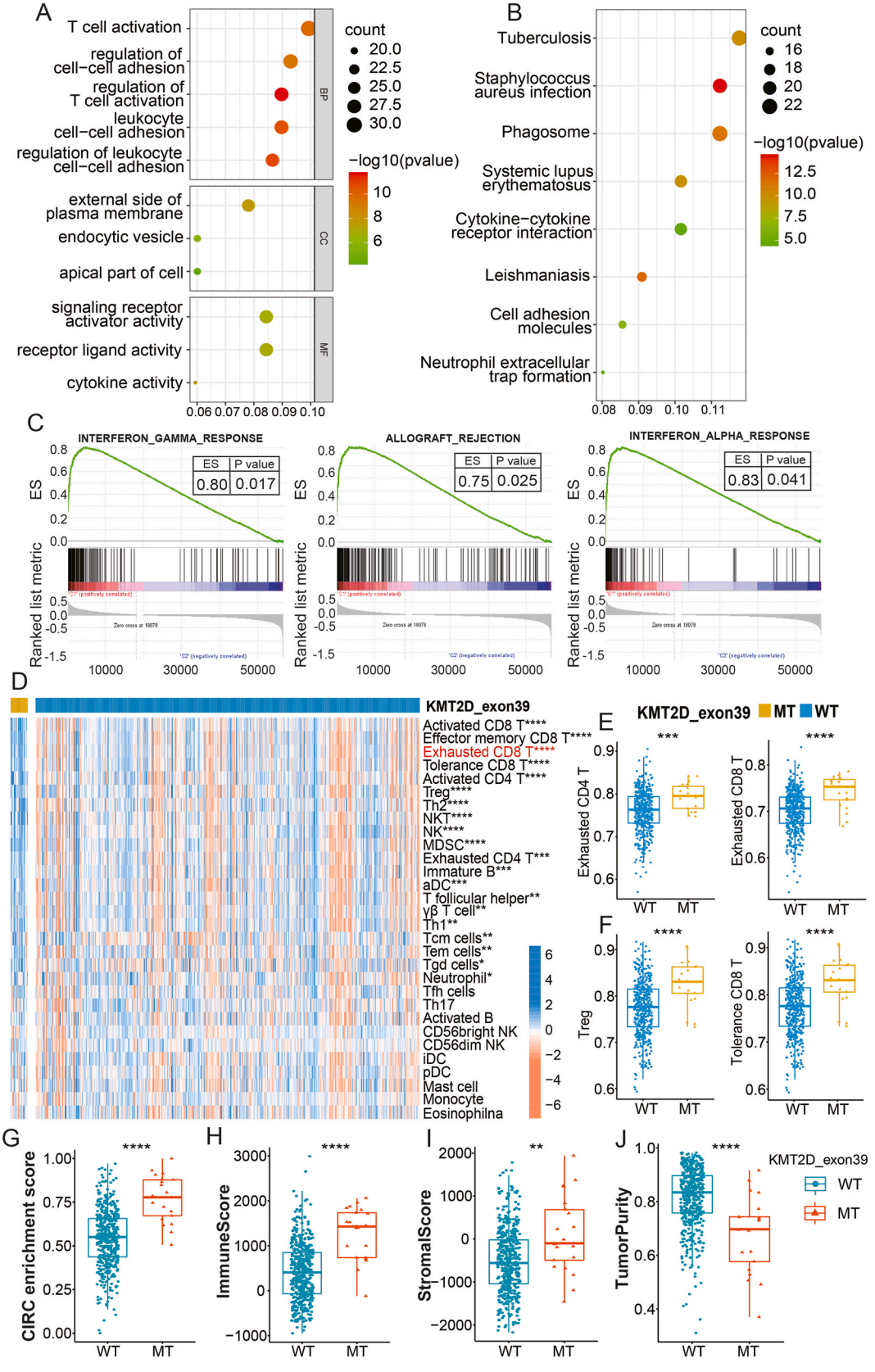

(caption on next page)

Fig. 3. (A–B) GO enrichment analysis and KEGG pathway analysis of differential genes between K-ex39^{MT} and K-ex39^{WT}; **(C)** Representative pathways between K-ex39^{MT} and K-ex39^{WT} identified by GSEA analysis, mainly related to immunity; **(D)** Heatmap of immune infiltrating cells in K-ex39^{MT} and K-ex39^{WT}; **(E–F)** Exhausted T cells, tolerance T cells and Treg cells in K-ex39^{MT} and K-ex39^{WT} patients; **(G–J)** CIRC enrichment score, immune scores, stromal scores, and tumor purity in K-ex39^{MT} and K-ex39^{WT} patients. K-ex39^{MT}: KMT2D exon 39 mutation type; K-ex39^{WT}: KMT2D exon 39 wild type; CIRC: Co-ordinate Immune Response Cluster.

2. Results

2.1. KMT2D^{MT} and K-ex39^{MT} in pan cancer

From the TCGA database, a total of 9072 patients of the above 21 malignancies were included, with 958 developing KMT2D^{MT} (Supplementary Table S3). We examined the ratio of the number and kind of mutations to learn more about how individuals with KMT2D^{MT} are affected by each cancer type. As depicted in Fig. 1A, uterine corpus endometrial cancer (UCEC) patients had the highest mutation rate (162/529, 30.6%), followed by bladder carcinoma (BLCA) patients (114/412, 27.67%) and lung squamous cell carcinoma (LUSC) patients (116/491, 23.63%), while ovarian carcinoma (OV) patients had the lowest mutation rate (6/436, 1.38%). Missense mutations were the most common type of tumor-causing mutation, accounting for the largest proportion of all 21 cancer types (Fig. S1A). Furthermore, only UCEC covers all six types of mutations.

To better understand the impact of KMT2D^{MT} on the prognosis of cancer patients, we mapped overall survival (OS) and excluded individuals with a survival time of fewer than 30 days. As illustrated in Fig. 1B, KMT2D^{MT} patients in the TCGA cohort had a longer OS (median OS 25 months versus 23.92 months, hazard ratio [HR] = 0.976 [95% CI: 0.846–1.012], $P = 0.693$). Nevertheless, in the MSK-IMPACT cohort, KMT2D^{WT} patients exhibited a longer OS (median OS 26.56 months vs 21.66 months, HR = 1.189 [95% CI:1.029–1.373], P = 0.018). The disparity in outcomes between the two cohorts prompted us to dig deeper into the reasons. Previous research has demonstrated that gene exon mutations cause carcinogenesis and alter cancer patient prognosis, such as the EGFR exon 20 mutation and the MET exon 14 mutation in lung cancer patients [23,24]. As a result, we study deeper into the KMT2D exon mutation. As shown in Fig. 1C and Fig. S1E, KMT2D^{MT} was mainly found in exon 31, exon 39, exon 10, and exon 48. We looked at the top six exons with the highest mutation rate, and found that while exon 31 and exon 39 had the highest mutation rate (Fig. 1D). A previous study illustrated that the frequency of nonsense mutation was the highest in KMT2D [25], which leads to the tumorigenesis. And exon 39 had the highest nonsense mutation rate, so we chose it for further study.

To further understand the role of K-ex39^{MT} in malignancies, we performed a prognostic analysis of patients with mutations in exon 39. In both the TCGA cohort and the MSK-IMPACT cohort, however, the difference in OS of patients with K-ex39^{MT} versus K-ex39^{WT} was not statistically significant (Figs. S1B and S1C). In each tumor, the inflammation score was compared between K-ex39^{MT} with K-ex39^{WT}, and the results showed that inflammatory scores differed in CRAD and LUSC. In detail, patients with K-ex39^{MT} had greater inflammation score than K-ex39^{WT} patients in CRAD, while K-ex39^{WT} patients had higher inflammation levels in LUSC (Fig. S1D), indicating that K-ex39^{MT} play diverse roles in various malignancies. To get a particular understanding of immune infiltration, Immune infiltration in patients with K-ex39^{MT} in 21 malignancies from individuals with K-ex39^{MT} in each cancer was measured. CRAD exhibited a greater degree of immune cell infiltration than other malignancies (Fig. 1E), further defining the relevance of K-ex39^{MT} in CRAD patients.

2.2. K-ex39^{MT} predicts worse prognosis, higher TMB and lower CNA in CRAD

To study further the differences between K-ex39^{MT} and K-ex39^{WT} in CRAD patients, we first conducted a survival analysis using the TCGA cohort (n = 477, the rate of K-ex39^{MT}: 3.56%). Patients with the K-ex39^{MT} showed a worse survival rate ($P = 0.083$) when compared to K-ex39^{WT} patients (Fig. 2A). Across sex, age, AJCC stage, N stage, TMB level, CNA level, and MSI status, the survival advantage of K-ex39^{WT} versus K-ex39^{MT} was identical (Fig. 2B). TMB levels, CNA levels, MSI status, and stage were subsequently compared between the K-ex39^{MT} and the K-ex39^{WT}, and it was shown that patients with K-ex39^{MT} showed higher levels of TMB but lower levels of CNA ($P < 0.0001$) (Fig. 2C and E). Furthermore, the proportion of MSI-H patients was higher in the K-ex39^{MT}, as was the proportion of patients with Stage I-II (Fig. 2D and F). Then, we obtained another cohort (MSK-Colorectal cancer). The results showed that KMT2D^{MT} showed higher levels of TMB but lower levels of CNA ($P < 0.0001$), and the proportion of MSI-H patients was higher in the KMT2D^{MT} ($P < 0.0001$) (Figs. S1E and S1G).

We separated patients into four groups based on their K-ex39^{MT} status and MSI status: K-ex39^{MT}MSI-H, K-ex39^{MT}MSI-L/MSS, K-ex39^{WT}MSI-H, and K-ex39^{WT}MSI-L/MSS. K-ex39^{WT}MSI-H individuals, as expected, had the longest OS of any group, andK-ex39^{WT} successfully identified patients with greater survival benefit among MSI-H patients (Fig. 2G). The same analysis was performed on CNAs, which were separated into high and low CNAs to divide CRAD patients into four groups combined with K-ex39^{MT} status. Notably, the K-ex39^{WT} predicted better survival in patients with high or low CNA (Fig. 2H).

2.3. K-ex39^{MT} is characterized by enriched immune infiltration in CRAD

The expression matrix of the TCGA cohort was used to analyze how K-ex39^{MT} alters gene expression and function in CRAD. The GO results show that the differentially expressed genes between K-ex39^{MT} and K-ex39^{WT} are mainly enriched in pathways such as T cell activation, regulation of cell-cell adhesion, and regulation of T cell activation, indicating that K-ex39^{MT} may affect immune infiltration

and tumor immune response (Fig. 3A). Besides, it was mostly enriched in the immune pathway in the KEGG enrichment study, confirming the influence of the K-ex39^{MT} on tumor immunity (Fig. 3B). A GSVA analysis was used to compare the functional differences between K-ex39^{MT} and K-ex39^{WT}patients. As shown in Fig. 3C, K-ex39^{MT} was involved in both innate and adaptive immune responses and allograft rejection (IFN-gamma, normalized enrichment score (NES) = 0.80, $P = 0.017$; allograft rejection, NES = 0.75, p = 0.025; IFN-alpha, NES = 0.83, $P = 0.041$). The preceding findings further implied that the mutation on K-ex39 mostly impacts CRAD patients' immunity.

Using a range of gene sets of immune cells, we examined the difference in their infiltration between K-ex39^{MT} and K-ex39^{WT}. Both activated tumor immunity (activated CD8$^+$ T cells, activated CD4$^+$ T cells and NK cells) and suppressor tumor immunity (Treg cells and exhausted T cells) were detected in K-ex39^{MT} samples, as illustrated in Fig. 3D. In K-ex39^{MT} patients, other regulatory and helper immune cells were also more prevalent (Fig. 3D). We additionally exhibit exhausted T cells, CD8$^+$ tolerance T cells, and Treg cells to further illustrate how different between the two groups of patients (Fig. 3E and F).

The CIRC signature encompasses a variety of inhibitory immune-related genes and is used to assess a patient's immune response [26]. The CIRC enrichment score of K-ex39^{MT} was much greater than that of K-ex39^{WT}, as shown in Fig. 3G, indicating a more immunosuppressive condition in K-ex39^{MT}. In addition, we utilized the ESTIMATE algorithm to quantify the immune

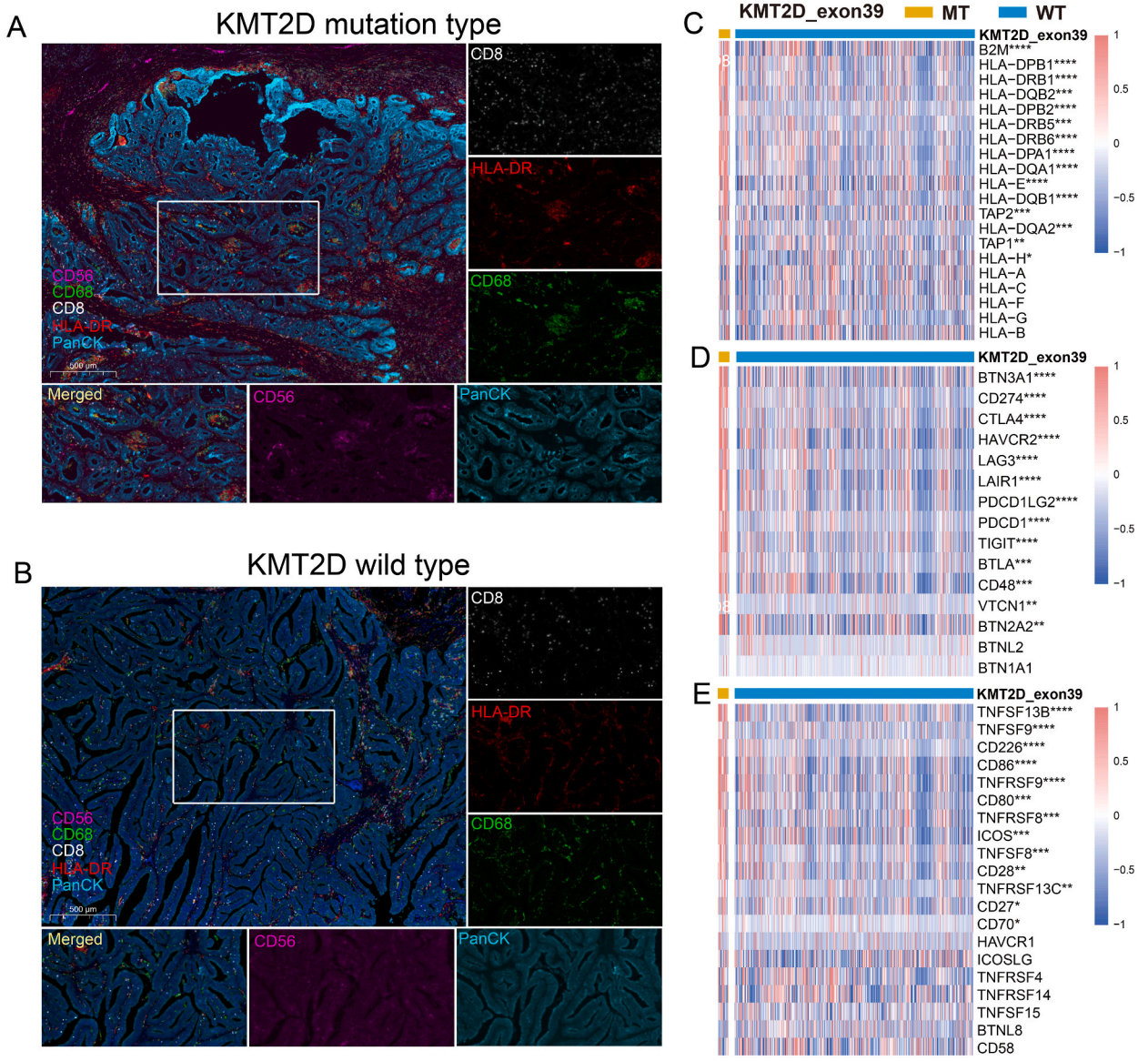

Fig. 4. **(A–B)** The expressions of CD68, CD56, CD8, HLA-DR and PanCK in KMT2D^{MT} and KMT2D^{WT} CRAD were detected by immunofluorescence. **(C–E)** Heatmap depicts immune-related gene expression levels in K-ex39^{MT} and K-ex39^{WT} patients. KMT2D^{MT}: mutation type; KMT2D^{WT}: KMT2D wild type; K-ex39^{MT}: KMT2D exon 39 mutation type; K-ex39^{WT}: KMT2D exon 39 wild type; CRAD: colorectal adenocarcinoma.

microenvironment of CRAD patients, and the results demonstrated that patients with K-ex39^{MT} had higher immune scores and stromal scores, but lower tumor purity, suggesting a higher degree of immune infiltration in patients with K-ex39^{MT} (Fig. 3H–J).

Due to the lack of detection of exon mutations, we selected KMT2D mutant and wild-type tissues for mIF. We compared the in-house CRAD sample between KMT2D^{MT} and KMT2D^{WT}. It showed that KMT2D^{MT} sample showed higher proportions of CD56, CD8, CD68 and HLA-DR, confirming the impact of KMT2D^{MT} on the immune microenvironment of CRAD patients (Fig. 4A and B). While the roles of K-ex39^{MT} in TME need to be confirmed further. We further analyzed immune-related gene expression in K-ex39^{MT} and K-ex39^{WT} and discovered that K-ex39^{MT} had higher MHC-related antigen-presenting molecules expression than K-ex39^{WT} (Fig. 4C). To compare immunomodulatory molecules in K-ex39^{MT} and K-ex39^{WT}, we employed a variety of co-stimulatory and co-inhibitory molecules. The results demonstrated that immunomodulatory molecules were expressed more in K-ex39^{MT} than in K-ex39^{WT} (most $P < 0.05$, Fig. 4D and E).

2.4. *Higher other mutations and immune-related genes expression in K-ex39^{MT}*

We examined K-ex39^{MT} and K-ex39^{WT} patients in the TCGA dataset to determine the genetic profile of CRAD patients and discovered many genes with considerably different mutation rates. The mutation rate in K-ex39^{MT} was greater than that of K-ex39^{WT} among several tumor-related pathway genes (such as the WNT pathway, JAK pathway, and NOTCH pathway) (Fig. 5A). Gens in other pathways, such as CCND3, ERBB2, FGFR2, KRAS, NRAS, EZH2, and PRDM1, had increased mutation rates in K-ex39^{WT} individuals but

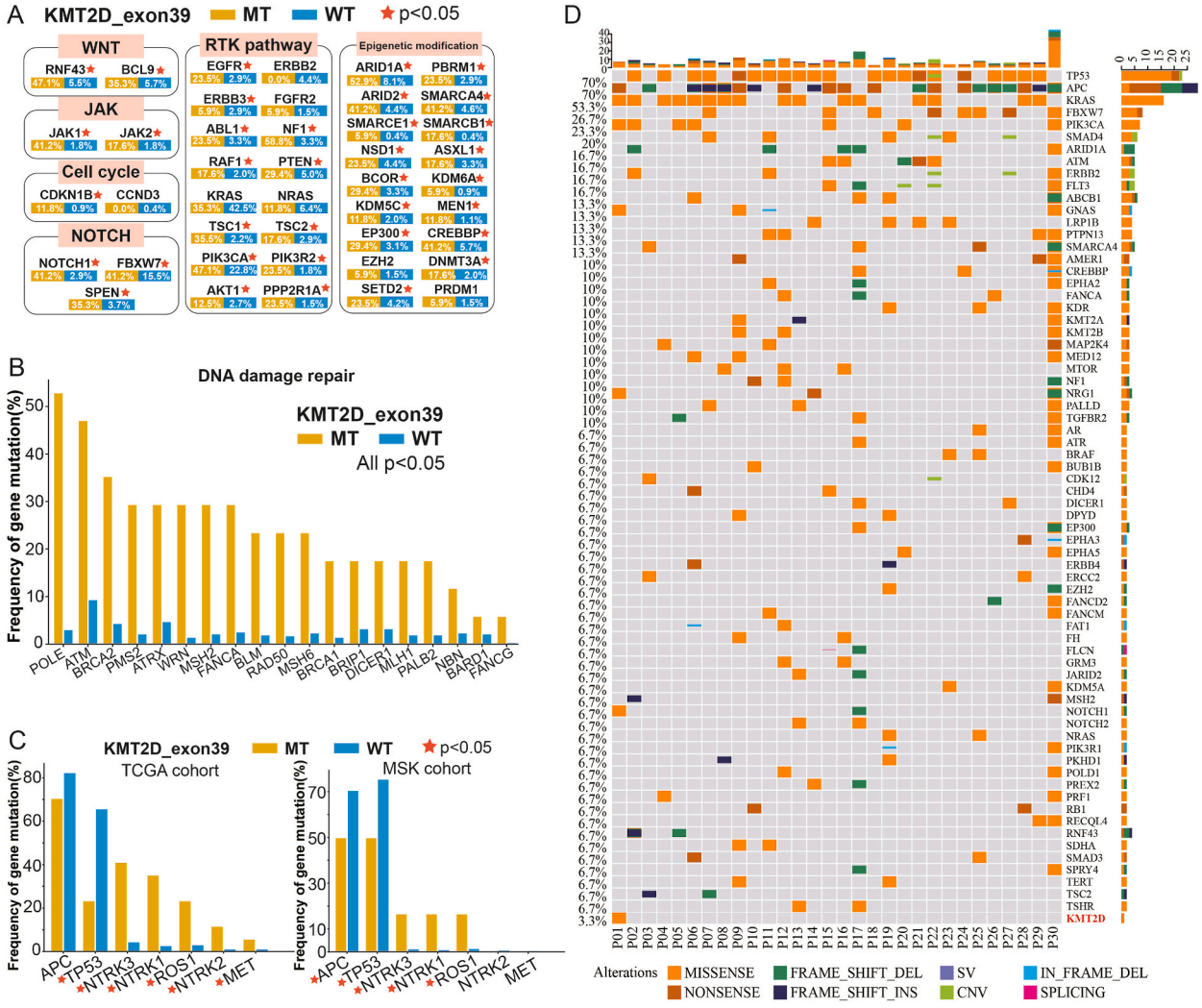

Fig. 5. **(A)** Comparison of gene mutation rates in the different pathways in K-ex39^{MT} and K-ex39^{WT}; **(B)** Comparison of gene mutation rates in the DDR pathway in K-ex39^{MT} and K-ex39^{WT}; **(C)** Comparison of common proto-oncogene and tumor suppressor gene mutations in CRAD patients between K-ex39^{MT} and K-ex39^{WT} patients; **(D)** The gene mutation status of 30 CRAD patients, and the incidence of KMT2D mutation was 3.3%. K-ex39^{MT}: KMT2D exon 39 mutation type; K-ex39^{WT}: KMT2D exon 39 wild type; CRAD: colorectal adenocarcinoma.

were not statistically significant ($P > 0.05$) (Fig. 5A). Genes with higher mutation rates in K-ex39^{MT} CRAD were mainly enriched in DNA damage repair (DDR) (such as POLE: 52.9% vs. 3.1%; BRCA2: 35.3% vs. 4.4%; MSH2: 29.4% vs. 2.2%); MSH6: 23.5% vs. 2.3%; MLH1: 17.6% vs. 2.0%; RAD50: 23.5% vs. 1.8%, all $P < 0.05$) (Fig. 5B). In addition, we investigated alterations in oncogenes and tumor suppressor genes that had been implicated in the genesis of CRAD cancers. As indicated in Fig. 5C, tumor suppressor genes (APC, TP53) had a greater mutation rate in K-ex39^{WT}, whereas oncogenes had a higher mutation rate in K-ex39^{MT}, and both results were similar in the TCGA and MSK-IMPACT cohorts. Then, among the 30 in-house CRAD patients, TP53, APC and KRAS were the most frequently mutated genes, and three of them had KMT2D mutation (Fig. 5D). The results validated that KMT2D^{MT} patients has lower APC and TP53 mutation.

2.5. K-ex39^{MT} is more sensitive to some chemotherapies but less to cetuximab

Following the determination of the influence of K-ex39^{MT} on the immunological milieu of CRAD patients, it was reported that genetic mutations also affect the patient's treatment sensitivity. To further investigate the impact of K-ex39^{MT} on treatment, we predicted the sensitivity of targeted therapy and chemotherapy in both K-ex39^{MT} and K-ex39^{WT} patients. IPRES signatures are composed of genes that regulate interstitial transition, cell adhesion, ECM remodeling, angiogenesis, and wound healing, and their high enrichment signals that patients may be resistant to immunotherapy. We compared IPRES signatures in K-ex39^{MT} and K-ex39^{WT} patients, and found that approximately half of the signatures were enriched in K-ex39^{MT} patients (such as Poola invasive breast cancer UP and MS RESP to wounding UP in MAPKi aPDL1 NR, $P < 0.05$) (Fig. 5A). In K-ex39^{MT} patients, the rest of the signatures showed no significant differences (Fig. 6A). Furthermore, we compared K-ex39^{MT} and K-ex39^{WT} patients using genes from multiple immune pathways, as described by Ryul et al. [27]. T cell infiltration and costimulatory pathways (anti-inflammatory and immunomodulatory) were considerably enriched in K-ex39^{MT} samples ($P < 0.05$), implying that K-ex39^{MT} activates immune cells (Fig. 6A). The TIDE algorithm can generate two scores (dysfunction score and exclusion score) that are used to assess tumor patients' immune function and

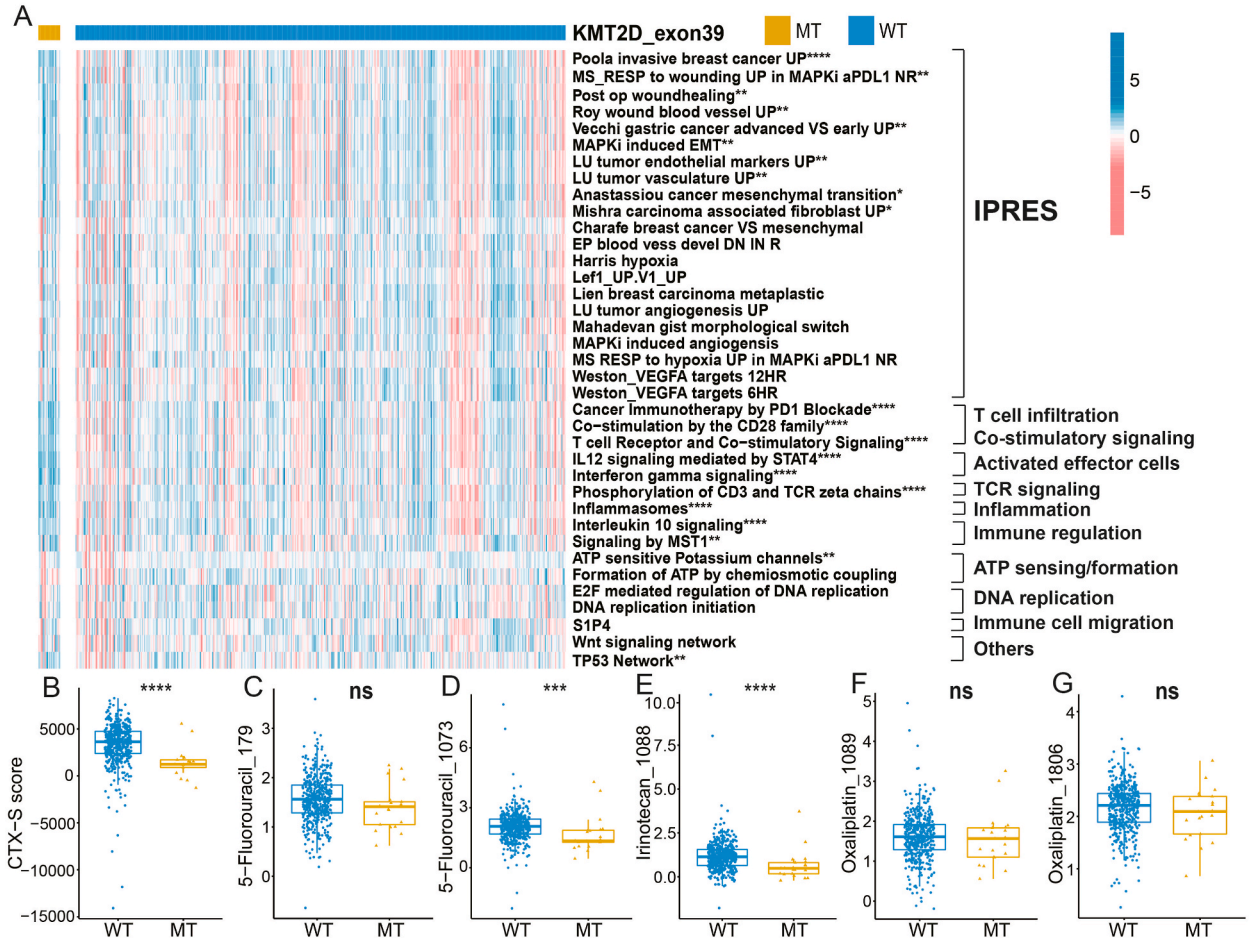

Fig. 6. **(A)** IPRES signature and immune-related pathways described by Ryul et al. in K-ex39^{MT} and K-ex39^{WT} patients; **(B)** CTX-S score in K-ex39^{MT} and K-ex39^{WT} patients; **(C–G)** IC50 of chemotherapies in K-ex39^{MT} and K-ex39^{WT} patients. K-ex39^{MT}: KMT2D exon 39 mutation type; K-ex39^{WT}: KMT2D exon 39 wild type; CTX-S: Cetuximab Sensitivity.

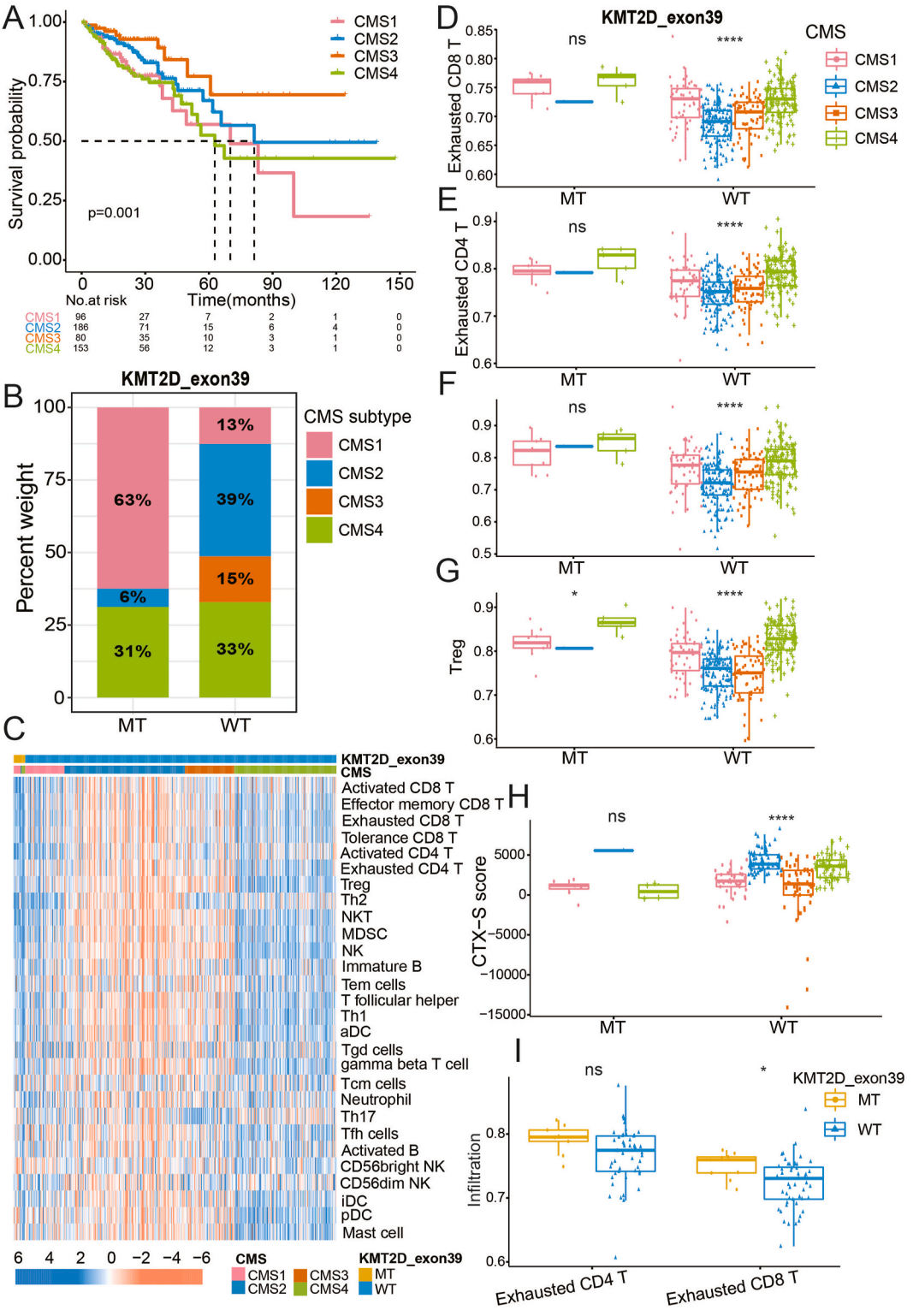

(caption on next page)

Fig. 7. Combined with CMS subtype of K-ex39^{MT} in CRAD; **(A)** Kaplan-Meier curves of OS of CMS subtype in CRAD patients; **(B)** Proportion of CMS subtype in K-ex39^{MT} and K-ex39^{WT} patients; **(C)** Immune infiltration in different CMS subtype in K-ex39^{MT} and K-ex39^{WT} patients; **(D–G)** Exhausted T cells, tolerance T cells and Treg cells in different CMS subtype in K-ex39^{MT} and K-ex39^{WT} patients; **(H)** CTX-S score in different CMS subtype in K-ex39^{MT} and K-ex39^{WT} patients; **(I)** Exhausted T cells in different CMS subtype in K-ex39^{MT} and K-ex39^{WT} patients. CMS: Consensus molecular subtype; CRAD: colorectal adenocarcinoma; K-ex39^{MT}: KMT2D exon 39 mutation type; K-ex39^{WT}: KMT2D exon 39 wild type; CTX-S: Cetuximab Sensitivity.

immune escape status, and hence indirectly measure the response to ICIs. Although there was no significant difference in the exclusion score, the dysfunction score was greater in K-ex39^{MT} patients, indicating a stronger immune evasion ability (Fig. S2A). Patients with timely mutations also had more tumor-infiltrating cytotoxic T cells, but they also had higher T cell dysfunction.

Molecularly targeted medicines and chemotherapy have always been important strategies for tumor treatment, notwithstanding the increased emphasis on immunotherapy in recent years. Given cetuximab is a typically targeted medication for patients with advanced CRAD, we used the CTX-S score to predict CTX sensitivity in K-ex39^{MT} patients. The findings revealed that K-ex39^{WT} patients were more susceptible to CTX and benefited from it (Fig. 6B), implying that K-ex39^{MT} patients may be resistant to EGFR inhibitors, which could be related to EGFR and RAS mutations in K-ex39^{MT} patients. In a previous study, it was found that APC and TP53 mutations can cause an increase in CTX-S score. While in our study, the mutation rates of APC and TP53 in K-ex39^{WT} patients were higher than those in K-ex39^{MT} patients, and the two conclusions were consistent.

The Genomics of Drug Sensitivity in Cancer (GDSC) database [28] was then utilized to predict CRAD sensitivity to routinely used chemotherapeutic medicines such as 5-Fluorouracil, irinotecan and oxaliplatin. 5-Fluorouracil and irinotecan IC50 were shown to be lower in K-ex39^{MT} patients, indicating that they are more sensitive to these two chemotherapeutics. In the case of oxaliplatin, however, there was no significant difference between K-ex39^{MT} and e K-ex39^{WT} patients (Fig. 6C–G).

2.6. *CMS subtypes differ in K-ex39^{MT} and K-ex39^{WT} patients*

According to CMS molecular typing, CRAD patients can be divided into CMS1 (microsatellite instability, immune type); CMS2 (typical, WNT and MYC signaling activation); CMS3 (metabotype, metabolic dysregulation) and CMS4 (mesenchymal type, transformed growth factor-beta activation and angiogenesis) [29]. We used prognostic analysis on the four categories of patients in the TCGA cohort to further understand the CMS categorization characteristics of CRAD patients (Fig. 7A). The results revealed that CMS3 patients had the longest OS, followed by CMS2. The CMS features of K-ex39^{MT} and K-ex39^{WT} patients were then compared. As shown in Fig. 7B, in the two groups of patients, the proportions of CMS1, CMS2 and CMS3 types were significantly different (CMS1: 63% vs. 13%; CMS2: 6% vs. 39%; CMS3: 0% vs. 15%).

We separated the patients into seven groups based on their KMT2D exon 39 mutant status and CMS classification, with no CMS3 type in the KMT2D exon 39 mutation patients. We used a heat map to depict the differences between the seven groups' immune cell infiltration in order to better comprehend them (Fig. 7C). Immune cell infiltration was substantially higher in K-ex39^{MT} patients than in K-ex39^{WT} patients. CMS4 and CMS1 patients' immune cells were higher enriched in K-ex39^{WT} individuals. We employ a violin diagram to help us grasp the exhausted T cells, CD8^{+} tolerance T cells, and Treg cells in the seven patient groups (Fig. 7D–G). CMS1, CMS2, and CMS4 were not statistically different among patients with K-ex39^{MT}, but CMS4 was considerably higher and CMS3 was the lowest among K-ex39^{WT} patients. Among the patients with CMS1, K-ex39^{MT} showed more infiltration of exhausted CD8 T cells ($P < 0.05$, Fig. 7I).

Finally, we analyzed CTX-score differences among CRAD patients, and discovered that CMS2 patients had the highest CTX-score, while CMS1 patients had the lowest, indicating that CMS2 patients were the most CTX-sensitive (Fig. 7H). We also compared chemosensitivity, dysfunction score and exclusion score among the seven patient groups. CMS4 patients exhibited the lowest sensitivity for both chemotherapy and immune escape ratings, despite the fact that there was no statistical difference between CMS1 and CMS4 in K-ex39^{MT} patients (Figs. S2B–S2F). CMS4 patients are the least susceptible among K-ex39^{WT} patients, while CMS3 patients may be more sensitive to chemotherapy and more effective for ICIs (Figs. S2B–S2F).

3. Discussion

Gene exon mutations are key causes of cancers, such as EGFR exon 20 deletion mutation and MET exon 14 mutation. The KMT2D mutation is a common mutation in cancer [30], and its exon 39 mutation has yet to be evaluated in CRAD patients. To investigate more, we assessed the significance of K-ex39^{MT} in 21 malignancies and their impact on immune infiltration and inflammatory scores. Furthermore, although not statistically significant, individuals with K-ex39^{MT} had a worse prognosis than patients with K-ex39^{WT}. Patients with K-ex39^{MT} had an immunosuppressive milieu and increased expression of a variety of immune-related genes, according to our findings. Moreover, we discovered that K-ex39^{MT} patients are more likely to produce immunological escape and resistance to immunotherapy, but are relatively more susceptible to chemotherapy when comparing the drug sensitivity prediction of K-ex39^{MT} and K-ex39^{WT}.

KMT2D is an epigenetic regulator, and the encoded protein is a histone methyltransferase, which has been linked to cancer in earlier research [31]. KMT2D has a vital function in promoting epidermal differentiation and ferroptosis, according to Shaun et al. and mice lacking epidermal KMT2D exhibited hallmarks of human precancerous tumors as well as altered the expression of essential genes and ferroptosis markers [32]. KMT2D^{MT} is linked to the production of early normal epithelial tissue, and it is more pronounced in

squamous cell carcinoma and basal cell carcinoma than in normal tissue [33,34]. The KMT2D^{MT} was discovered to influence the prognosis of tumor patients in our investigation. Although the results of the TCGA and MSK cohorts are inconsistent, we cannot rule out the possibility of exon mutation, thus we chose to conduct a particular exon analysis. Previous research on KMT2D exon mutations had been limited to Kabuki syndrome [35,36], with few breakthrough discoveries in cancer. A prior study discovered that missense mutations in exon 39 of KMT2D cause a new polymorphic disease separate from Kabuki syndrome, demonstrating the exon's specificity [37]. Exon 39 was chosen for additional investigation because it contains the highest proportion of missense and nonsense mutations in the KMT2D exon. Among 21 multiple solid tumors, the exon 39 mutation frequency is relatively high in CRAD, which means its importance. And we also found that samples with K-ex39^{MT} in CRAD were more enriched in preliminary results of immune infiltrating cells and inflammatory scores, indicating that K-ex39^{MT} had a greater impact on CRAD, thus we did more investigation on it.

We discovered gene mutations in epigenetic regulation, RTK/MAPK/PI3K, and DDR pathways when screening for genes that co-occur with K-ex39 alterations. RNAPII transcriptional elongation/transcriptional stress is a common hallmark of KMT2D^{MT} cancer cells, which explains the link between histone modifier gene alterations and KMT2D^{MT}. Indeed, epigenetic alterations provide intriguing novel targets for anticancer therapy, such as Tazemetostat, a histone methyltransferase inhibitor that has been shown to be effective in refractory B-cell non-Hodgkin lymphoma and epithelioid sarcoma [38]. The mutation rate of genes in both the ARID1A and DDR pathways was higher in patients with K-ex39^{MT}, showing that it plays an essential role in DNA repair function, which is consistent with earlier research [21,39]. We recognize that mutations in genes in the RTK/MAPK/PI3K pathway cause anticancer treatment resistance based on prior publications [40]. Genes like EGFR had considerably higher mutation rates in this study, however, more research is needed to determine whether CRAD with the K-ex39^{MT} is responsive to MAPK/PI3K pathway inhibitors. In addition to gene mutations in tumor-related pathways that are associated with K-ex39^{MT}, their relationship with frequent gene mutations in CRAD patients is investigated in further detail. APC and TP53, which are frequent tumor suppressor genes in CRAD, had greater mutation rates in K-ex39^{WT}, implying that K-ex39^{MT} negatively influences both.

As immunotherapy has gradually become an important treatment for CRAD in recent years, it has brought prognostic benefits to patients, such as anti-PD-1 antibody and anti-PD-L1 antibody [41,42]. Our results showed that K-ex39^{MT} is associated with markers of immunotherapy efficacy, including MSI, TMB, PD-L1 expression, and immune cell infiltration. In patients with K-ex39^{MT}, TMB was higher, which may be related to the high mutation rate of other genes. Recently, Wang et al. using CRISPR-GEMM, found that KMT2D is the main mechanism for blocking immune checkpoints by recruiting antigen-presenting cells and T cells [22], but more studies are needed to confirm the predicted value of K-ex39^{MT} on the efficacy of immunotherapy. Interestingly, immunosuppressive cells and immune co-suppressive molecules, including exhausted T cells and Treg cells, were significantly elevated in patients with K-ex39^{MT} compared with K-ex39^{WT}. Furthermore, both IPRES signatures and TIDE results imply that K-ex39^{MT} may promote immunological escape, resulting in immunotherapy resistance, and several studies have verified their predictive potential [43–45]. In addition to immunotherapy, K-ex39^{MT} patients are resistant to EGFR inhibitors, indicating that the K-ex39^{MT} diminishes the effectiveness of the patient's treatment and consequently impacts the patient's prognosis. We investigated the therapeutic sensitivity of K-ex39^{MT} patients combined with CMS typing, and the results showed that CMS4 patients were the least responsive to the three therapies, regardless of whether they were K-ex39^{MT} or K-ex39^{WT}. CMS4 has been demonstrated to have a bad prognosis in earlier investigations [46], which is consistent with the findings of this study. CMS3 paired with wild patients had the highest treatment sensitivity and could be utilized as a predictive marker in the future, but the treatment cohorts are needed to validate the results further.

In conclusion, we confirmed that KMT2D^{MT} and K-ex39^{MT} play an essential role in CRAD. CRAD patients with K-ex39^{MT} have more abundant immune cell infiltration and enrichment of immune-related pathways and signatures, which suggested its predictive role in immunotherapy response. Besides, K-ex39^{MT} CRAD patients may be more sensitive to some chemotherapies but less to cetuximab.

4. Material and methods

4.1. Data of patients

Mutation and RNA-seq data (FPKM) for 21 selected solid tumors with a clear diagnosis (cancer types are described in Supplementary Table S1) were obtained from TCGA (https://www.portal.gdc.cancer.gov/) and the accompanying clinical data were gathered from cBioPortal (https://cbioportal.org/). In addition, the mutation and follow-up data from the MSK-IMPACT cohort of the same cancer types and MSK-Colorectal cancer were retrieved from cBioPortal [47,48]. In this study, KMT2D^{MT} was classified as patients who had mutations in the KMT2D gene, whereas KMT2D wild (KMT2D^{WT}) was characterized as patients who did not have KMT2D gene mutations but may be accompanied by other gene mutations. K-ex39^{MT} was defined as a mutation that only appeared in exon 39 of KMT2D, whereas KMT2D exon39 wild (K-ex39^{WT}) was defined as no mutation in any exon of the KMT2D gene, and patients with mutations in other exons were excluded.

The resected 30 CRAD patient tissues were obtained from the First Affiliated Hospital, Zhejiang University School of Medicine from 2018 to 2021, which were fixed with 4% paraformaldehyde before embedding in paraffin. And this study was approved by the Ethics Committee of the First Affiliated Hospital, Zhejiang University School of Medicine.

4.2. Gene sequencing, TMB and CNA data analysis

On the HiSeq4000 platform (Illumina), the target enriched libraries were sequenced using 2150 bp pair-end reads. Demultiplexing the sequencing data with bcl2fastq (version 2.19) was followed by analysis with Trimmomatic to weed out low-quality (quality 15) or

N bases. Burrows-Wheeler Aligner (bwa-mem) was used to align the data to the hg19 reference human genome, and the Picard suite (found at: https://broadinstitute.github.io/picard/) and Genome Analysis Toolkit were then used to process the results (GATK). The mutant allele frequency cut-off was set at 0.5% for calling SNPs and indels in GATK using VarScan228 and HaplotypeCaller/UnifiedGenotyper. The 1000 Genome Project and dbSNP were used to exclude frequent variations. By contrasting with patient whole blood controls, germline mutations were eliminated.

TMB stands for the total amount of coding errors, base substitutions, gene insertion and deletion errors per megabase (Mb) of the discovered somatic gene after germline mutations have been eliminated from the tumor genome. Recent evidence indicates that TMB influences the therapeutic efficacy of ICIs, suggesting its usage as a biomarker of efficacy. There is no clearly defined threshold for high and low TMB, and the cutoff value for high and low TMB in this investigation was the highest 20% of TMB in all cancer samples of TCGA cohort [49].

CNA data from the TCGA cohort and MSK-IMPACT cohort were retrieved from the cBioPortal and characterized as the proportion of copy number changed genomes. The median of all cancer samples was used as the cutoff value for CNA.

4.2. Immune-related functional enrichment analysis

To study the infiltration status of immune cells, we evaluated K-ex39^{MT} samples of each cancer type and compared K-ex39^{MT} with K-ex39^{WT} of CRAD patients in the TCGA cohort using the ssGSEA algorithm [50]. The "GSVA" package was used to generate the inflammation score, and normalized enrichment scores and immune cell signatures were gathered and summarized in Supplementary Table S2. Among them, previous investigations had provided gene sets for exhausted T cells and tolerance T cells.

To further explore the enrichment characteristics of in patients with K-ex39^{MT}, we analyzed the differential gene expression of K-ex39^{MT} and K-ex39^{WT} patients using the "DESeq2" package and performed the Kyoto Encyclopedia of Genes and Genomes (KEGG) pathway and Gene Ontology (GO) enrichment analyses. Meanwhile, gene set enrichment analysis (GSEA) software was used to perform GSEA [51] with nominal *P* value, and the ESTIMATE method was used to characterize the tumor microenvironment, which included immune score, stromal score, and tumor purity [52]. In addition, we also compared the Co-ordinate Immune Response Cluster (CIRC) signature [53] and Innate anti-PD-1 Resistance (IPRES) signature [54] between K-ex39^{MT} and K-ex39^{WT}, which are related to tumor immune responses. Additionally, the expression of immune-related genes was compared between K-ex39^{MT} and K-ex39^{WT}, based on the functional classification of Thorsson et al. [55].

4.3. Multiple immunofluorescences (mIF)

The resected CRAD patient tissues were obtained from the First Affiliated Hospital, Zhejiang University School of Medicine. The prepared tissue sections (4 μm) were dewaxed with xylene and rehydrated with graded alcohol, and chose a K-ex39^{MT} tissue and a K-ex39^{WT} tissue to accomplish mIF to identify a series of immune cells (such as T cells, and NK cells) (panel: CD68, CD56, CD8, HLA-DR, PanCK). Tissue sections were treated with goat serum blocking solution (WiSee Biotechnology, A10015-100, China) for 1 h at room temperature before exposing them to the primary and secondary antibodies for an additional 30 min at room temperature (the primary antibodies: CD8, 1:300, BX50036-C3; CD68, 1:400, BX50031; CD56, 1:100, #3576, HLA-DR, 1:1000, ab92511, PanCK, 1x, GM351507. The fluorescent secondary antibodies: Neon TSA620, Neon TSA570, Neon TSA670, Neon TSA440, 1:100). Tissue samples were stained using an IHC assay kit (WiSee Biotechnology, DS9800, China) according to the manufacturer's instructions. Mounted sections were examined by light microscopy (Leica, Germany), and Halo software was used to analyze the captured pictures (Indica Lab, USA, version 3.3).

4.4. Prediction of the sensitivity to different treatments

The Cetuximab Sensitivity (CTX-S) score is based on the gene expression values of 800 cancer-related genes, and the details on the score's derivation and validation have already been disclosed [56]. The R package of "oncoPredict" was used to estimate the 50% inhibiting concentration (IC50) of chemotherapeutic and targeted therapy for CRAD, where IC50 refers to a substance's ability to inhibit a specific biological or metabolic activity [57]. The clinical response of CRAD patients to immunotherapy was predicted using the Tumor Immune Dysfunction and Exclusion (TIDE) algorithm (http://tide.dfci.harvard.edu/) [44].

4.5. CMS analysis

The Consensus molecular subtype (CMS) system is currently the most comprehensive and influential molecular subtype model for CRAD. Using network clustering analysis, it separates CRAD into four CMS molecular kinds based on the massive data from six independent CRAD sequencing projects in the past [29]. We employed the "CMScaller" algorithm to perform CMS categorization of CRAD samples applying gene expression data from CRAD patients in TCGA [58].

4.6. Statistical analysis

R software (version4.1.1) or SPSS (version 25.0) were used for all statistical analyses. The OS curve was drawn using the Kaplan-Meier survival analysis, and the significance of the curve was determined using the log-rank test. Cox proportional hazards models were used to perform multivariate survival analyses that were adjusted for available confounders, including age, sex, AJCC stage, N

stage, TMB level, CNA level, and MSI status. Differential expression genes were defined as those with adjusted $P < 0.01$ and $|\text{LogFC}| > 1.5$. TMB, CNA, IC50, tumor immune cells, gene expression, and gene signatures in K-ex39^{MT} and K-ex39^{WT} samples were compared using the Mann-Whitney test.

5. Limitations of the study

There are several limitations to this research. First, KMT2D^{MT} was shown to be associated with immunotherapy efficacy in cholangiocarcinoma [59,60], while the role in CRAD requires further validation in other cohorts. Second, while the sample size of the K-ex39^{MT} is limited, it is prone to statistical significance when performing survival and immunotherapy response correlation analyses, which should be confirmed in bigger samples. Finally, further immunotherapy cohorts and trials are required to confirm the effects of K-ex39^{MT} on immunotherapy.

Author contribution

Peng Zhao, Xuanwen Bao and Chuan Liu conceived and designed the experiments. Chuan Liu and Xuanwen Bao performed the experiments. Chuan Liu and Xuanwen Bao analyzed and interpreted the data. Yuzhi Jin, Yixuan Guo, Hangyu Zhang and Junrong Yan contributed reagents, materials, analysis tools or data. Chuan Liu and Hangyu Zhang wrote the paper.

Declaration of competing interest

The authors declare no competing interests.

Data availability statement

Data included in article/supp. material/referenced in article.

Funding statement

This work was supported by the National Natural Science Foundation of China 82101830 (X.B.), 81472346 (P.Z.), 82074208 (P.Z.), by the Natural Science Foundation of Zhejiang Province LY20H160033 (P.Z.).

Acknowledgments

None.

Appendix A. Supplementary data

Supplementary data to this article can be found online at https://doi.org/10.1016/j.heliyon.2023.e13629.

References

[1] K.N. Berger, J.J. Pu, PD-1 pathway and its clinical application: a 20year journey after discovery of the complete human PD-1 gene, Gene 638 (2018) 20–25, https://doi.org/10.1016/j.gene.2017.09.050.
[2] R.J. Kelly, J.A. Ajani, J. Kuzdzal, et al., Adjuvant nivolumab in resected esophageal or gastroesophageal junction cancer, N. Engl. J. Med. 384 (13) (2021) 1191–1203, https://doi.org/10.1056/NEJMoa2032125.
[3] H.A. Tawbi, P.A. Forsyth, A. Algazi, et al., Combined nivolumab and ipilimumab in melanoma metastatic to the brain, N. Engl. J. Med. 379 (8) (2018) 722–730, https://doi.org/10.1056/NEJMoa1805453.
[4] O. Hamid, C. Robert, A. Daud, et al., Safety and tumor responses with lambrolizumab (anti-PD-1) in melanoma, N. Engl. J. Med. 369 (2) (2013) 134–144, https://doi.org/10.1056/NEJMoa1305133.
[5] P.A. Ott, Y.J. Bang, S.A. Piha-Paul, et al., T-Cell-Inflamed gene-expression profile, programmed death ligand 1 expression, and tumor mutational burden predict efficacy in patients treated with pembrolizumab across 20 cancers: KEYNOTE-028, J. Clin. Oncol. 37 (4) (2019) 318–327, https://doi.org/10.1200/jco.2018.78.2276.
[6] R. Bonneville, M.A. Krook, E.A. Kautto, et al., Landscape of microsatellite instability across 39 cancer types, JCO Precis Oncol (2017) 2017, https://doi.org/10.1200/po.17.00073.
[7] M.J. Overman, R. McDermott, J.L. Leach, et al., Nivolumab in patients with metastatic DNA mismatch repair-deficient or microsatellite instability-high colorectal cancer (CheckMate 142): an open-label, multicentre, phase 2 study, Lancet Oncol. 18 (9) (2017) 1182–1191, https://doi.org/10.1016/s1470-2045(17)30422-9.
[8] X. Bao, H. Zhang, W. Wu, et al., Analysis of the molecular nature associated with microsatellite status in colon cancer identifies clinical implications for immunotherapy, J. Immunother. Can. 8 (2) (2020), https://doi.org/10.1136/jitc-2020-001437.
[9] T. Davoli, H. Uno, E.C. Wooten, S.J. Elledge, Tumor aneuploidy correlates with markers of immune evasion and with reduced response to immunotherapy, Science 355 (6322) (2017), https://doi.org/10.1126/science.aaf8399.
[10] A.A. Hakimi, M.H. Voss, F. Kuo, et al., Transcriptomic profiling of the tumor microenvironment reveals distinct subgroups of clear cell renal cell cancer: data from a randomized phase III trial, Cancer Discov. 9 (4) (2019) 510–525, https://doi.org/10.1158/2159-8290.cd-18-0957.

[11] A. Marabelle, D.T. Le, P.A. Ascierto, et al., Efficacy of pembrolizumab in patients with noncolorectal high microsatellite instability/mismatch repair-deficient cancer: results from the phase II KEYNOTE-158 study, J. Clin. Oncol. 38 (1) (2020) 1–10, https://doi.org/10.1200/jco.19.02105.

[12] T.S.K. Mok, Y.L. Wu, I. Kudaba, et al., Pembrolizumab versus chemotherapy for previously untreated, PD-L1-expressing, locally advanced or metastatic non-small-cell lung cancer (KEYNOTE-042): a randomised, open-label, controlled, phase 3 trial, Lancet 393 (10183) (2019) 1819–1830, https://doi.org/10.1016/s0140-6736(18)32409-7.

[13] P.J. Roberts, T.E. Stinchcombe, KRAS mutation: should we test for it, and does it matter? J. Clin. Oncol. 31 (8) (2013) 1112–1121, https://doi.org/10.1200/jco.2012.43.0454.

[14] S.A. Kerk, T. Papagiannakopoulos, Y.M. Shah, C.A. Lyssiotis, Metabolic networks in mutant KRAS-driven tumours: tissue specificities and the microenvironment, Nat. Rev. Cancer 21 (8) (2021) 510–525, https://doi.org/10.1038/s41568-021-00375-9.

[15] H. Yasuda, S. Kobayashi, D.B. Costa, EGFR exon 20 insertion mutations in non-small-cell lung cancer: preclinical data and clinical implications, Lancet Oncol. 13 (1) (2012) e23–e31, https://doi.org/10.1016/s1470-2045(11)70129-2.

[16] S. Vyse, P.H. Huang, Targeting EGFR exon 20 insertion mutations in non-small cell lung cancer, Signal Transduct. Targeted Ther. 4 (2019) 5, https://doi.org/10.1038/s41392-019-0038-9.

[17] H. Alam, M. Tang, M. Maitituoheti, et al., KMT2D deficiency impairs super-enhancers to confer a glycolytic vulnerability in lung cancer, Cancer Cell 37 (4) (2020) 599–617.e597, https://doi.org/10.1016/j.ccell.2020.03.005.

[18] A. Augert, Q. Zhang, B. Bates, et al., Small cell lung cancer exhibits frequent inactivating mutations in the histone methyltransferase KMT2D/MLL2: CALGB 151111 (alliance), J. Thorac. Oncol. 12 (4) (2017) 704–713, https://doi.org/10.1016/j.jtho.2016.12.011.

[19] C.S. Grasso, Y.M. Wu, D.R. Robinson, et al., The mutational landscape of lethal castration-resistant prostate cancer, Nature 487 (7406) (2012) 239–243, https://doi.org/10.1038/nature11125.

[20] The molecular taxonomy of primary prostate cancer, Cell 163 (4) (2015) 1011–1025, https://doi.org/10.1016/j.cell.2015.10.025.

[21] T. Kantidakis, M. Saponaro, R. Mitter, et al., Mutation of cancer driver MLL2 results in transcription stress and genome instability, Genes Dev. 30 (4) (2016) 408–420, https://doi.org/10.1101/gad.275453.115.

[22] G. Wang, R.D. Chow, L. Zhu, et al., CRISPR-GEMM pooled mutagenic screening identifies KMT2D as a major modulator of immune checkpoint blockade, Cancer Discov. 10 (12) (2020) 1912–1933, https://doi.org/10.1158/2159-8290.cd-19-1448.

[23] J.H. Tong, S.F. Yeung, A.W. Chan, et al., MET amplification and exon 14 splice site mutation define unique molecular subgroups of non-small cell lung carcinoma with poor prognosis, Clin. Cancer Res. 22 (12) (2016) 3048–3056, https://doi.org/10.1158/1078-0432.ccr-15-2061.

[24] G.R. Oxnard, P.C. Lo, M. Nishino, et al., Natural history and molecular characteristics of lung cancers harboring EGFR exon 20 insertions, J. Thorac. Oncol. 8 (2) (2013) 179–184, https://doi.org/10.1097/JTO.0b013e3182779d18.

[25] B. Zheng, Z. Song, Y. Chen, W. Yan, Genomic analyses of metaplastic or sarcomatoid carcinomas from different organs revealed frequent mutations in KMT2D, Front. Mol. Biosci. 8 (2021), 688692, https://doi.org/10.3389/fmolb.2021.688692.

[26] G. Bindea, B. Mlecnik, M. Tosolini, et al., Spatiotemporal dynamics of intratumoral immune cells reveal the immune landscape in human cancer, Immunity 39 (4) (2013) 782–795, https://doi.org/10.1016/j.immuni.2013.10.003.

[27] R. Kim, M. An, H. Lee, et al., Early tumor-immune microenvironmental remodeling and response to first-line fluoropyrimidine and platinum chemotherapy in advanced gastric cancer, Cancer Discov. 12 (4) (2022) 984–1001, https://doi.org/10.1158/2159-8290.cd-21-0888.

[28] F. Iorio, T.A. Knijnenburg, D.J. Vis, et al., A landscape of pharmacogenomic interactions in cancer, Cell 166 (3) (2016) 740–754, https://doi.org/10.1016/j.cell.2016.06.017.

[29] J. Guinney, R. Dienstmann, X. Wang, et al., The consensus molecular subtypes of colorectal cancer, Nat. Med. 21 (11) (2015) 1350–1356, https://doi.org/10.1038/nm.3967.

[30] G. Mendiratta, E. Ke, M. Aziz, D. Liarakos, M. Tong, E.C. Stites, Cancer gene mutation frequencies for the U.S. population, Nat. Commun. 12 (1) (2021) 5961, https://doi.org/10.1038/s41467-021-26213-y.

[31] J.E. Lee, C. Wang, S. Xu, et al., H3K4 mono- and di-methyltransferase MLL4 is required for enhancer activation during cell differentiation, Elife 2 (2013), e01503, https://doi.org/10.7554/eLife.01503.

[32] S. Egolf, J. Zou, A. Anderson, et al., MLL4 mediates differentiation and tumor suppression through ferroptosis, Sci. Adv. 7 (50) (2021) eabj9141, https://doi.org/10.1126/sciadv.abj9141.

[33] J.C. Fowler, C. King, C. Bryant, et al., Selection of oncogenic mutant clones in normal human skin varies with body site, Cancer Discov. 11 (2) (2021) 340–361, https://doi.org/10.1158/2159-8290.cd-20-1092.

[34] R. Li, Y. Du, Z. Chen, et al., Macroscopic somatic clonal expansion in morphologically normal human urothelium, Science 370 (6512) (2020) 82–89, https://doi.org/10.1126/science.aba7300.

[35] P.K. Yamamoto, T.A. de Souza, A. Antiorio, et al., Genetic and behavioral characterization of a Kmt2d mouse mutant, a new model for Kabuki Syndrome, Gene Brain Behav. 18 (8) (2019), e12568, https://doi.org/10.1111/gbb.12568.

[36] E. Aref-Eshghi, D.K. Bourque, J. Kerkhof, et al., Genome-wide DNA methylation and RNA analyses enable reclassification of two variants of uncertain significance in a patient with clinical Kabuki syndrome, Hum. Mutat. 40 (10) (2019) 1684–1689, https://doi.org/10.1002/humu.23833.

[37] S. Cuvertino, V. Hartill, A. Colyer, et al., A restricted spectrum of missense KMT2D variants cause a multiple malformations disorder distinct from Kabuki syndrome, Genet. Med. 22 (5) (2020) 867–877, https://doi.org/10.1038/s41436-019-0743-3.

[38] A. Italiano, J.C. Soria, M. Toulmonde, et al., Tazemetostat, an EZH2 inhibitor, in relapsed or refractory B-cell non-Hodgkin lymphoma and advanced solid tumours: a first-in-human, open-label, phase 1 study, Lancet Oncol. 19 (5) (2018) 649–659, https://doi.org/10.1016/s1470-2045(18)30145-1.

[39] E.M. Je, S.H. Lee, N.J. Yoo, S.H. Lee, Mutational and expressional analysis of MLL genes in gastric and colorectal cancers with microsatellite instability, Neoplasma 60 (2) (2013) 188–195, https://doi.org/10.4149/neo_2013_025.

[40] S. Mitani, H. Kawakami, Emerging targeted therapies for HER2 positive gastric cancer that can overcome trastuzumab resistance, Cancers 12 (2) (2020), https://doi.org/10.3390/cancers12020400.

[41] F. Sclafani, MEK and PD-L1 inhibition in colorectal cancer: a burning blaze turning into a flash in the pan, Lancet Oncol. 20 (6) (2019) 752–753, https://doi.org/10.1016/s1470-2045(19)30076-2.

[42] L.A. Diaz Jr., K.K. Shiu, T.W. Kim, et al., Pembrolizumab versus chemotherapy for microsatellite instability-high or mismatch repair-deficient metastatic colorectal cancer (KEYNOTE-177): final analysis of a randomised, open-label, phase 3 study, Lancet Oncol. 23 (5) (2022) 659–670, https://doi.org/10.1016/s1470-2045(22)00197-8.

[43] P.K.H. Lau, B. Feran, L. Smith, et al., Melanoma brain metastases that progress on BRAF-MEK inhibitors demonstrate resistance to ipilimumab-nivolumab that is associated with the Innate PD-1 Resistance Signature (IPRES), J. Immunother. Can. 9 (10) (2021), https://doi.org/10.1136/jitc-2021-002995.

[44] P. Jiang, S. Gu, D. Pan, et al., Signatures of T cell dysfunction and exclusion predict cancer immunotherapy response, Nat. Med. 24 (10) (2018) 1550–1558, https://doi.org/10.1038/s41591-018-0136-1.

[45] J. Fu, K. Li, W. Zhang, et al., Large-scale public data reuse to model immunotherapy response and resistance, Genome Med. 12 (1) (2020) 21, https://doi.org/10.1186/s13073-020-0721-z.

[46] S. Ten Hoorn, T.R. de Back, D.W. Sommeijer, L. Vermeulen, Clinical value of consensus molecular subtypes in colorectal cancer: a systematic review and meta-analysis, J. Natl. Cancer Inst. 114 (4) (2022) 503–516, https://doi.org/10.1093/jnci/djab106.

[47] A. Zehir, R. Benayed, R.H. Shah, et al., Mutational landscape of metastatic cancer revealed from prospective clinical sequencing of 10,000 patients, Nat. Med. 23 (6) (2017) 703–713, https://doi.org/10.1038/nm.4333.

[48] S. Mondaca, H. Walch, S. Nandakumar, W.K. Chatila, N. Schultz, R. Yaeger, Specific mutations in APC, but not alterations in DNA damage response, associate with outcomes of patients with metastatic colorectal cancer, Gastroenterology 159 (5) (2020) 1975–1978.e1974, https://doi.org/10.1053/j.gastro.2020.07.041.

[49] R.M. Samstein, C.H. Lee, A.N. Shoushtari, et al., Tumor mutational load predicts survival after immunotherapy across multiple cancer types, Nat. Genet. 51 (2) (2019) 202–206, https://doi.org/10.1038/s41588-018-0312-8.
[50] D.A. Barbie, P. Tamayo, J.S. Boehm, et al., Systematic RNA interference reveals that oncogenic KRAS-driven cancers require TBK1, Nature 462 (7269) (2009) 108–112, https://doi.org/10.1038/nature08460.
[51] A. Subramanian, P. Tamayo, V.K. Mootha, et al., Gene set enrichment analysis: a knowledge-based approach for interpreting genome-wide expression profiles, Proc. Natl. Acad. Sci. U. S. A. 102 (43) (2005) 15545–15550, https://doi.org/10.1073/pnas.0506580102.
[52] K. Yoshihara, M. Shahmoradgoli, E. Martínez, et al., Inferring tumour purity and stromal and immune cell admixture from expression data, Nat. Commun. 4 (2013) 2612, https://doi.org/10.1038/ncomms3612.
[53] N. Lal, A.D. Beggs, B.E. Willcox, G.W. Middleton, An immunogenomic stratification of colorectal cancer: implications for development of targeted immunotherapy, OncoImmunology 4 (3) (2015), e976052, https://doi.org/10.4161/2162402x.2014.976052.
[54] W. Hugo, J.M. Zaretsky, L. Sun, et al., Genomic and transcriptomic features of response to anti-PD-1 therapy in metastatic melanoma, Cell 165 (1) (2016) 35–44, https://doi.org/10.1016/j.cell.2016.02.065.
[55] V. Thorsson, D.L. Gibbs, S.D. Brown, et al., The immune landscape of cancer, Immunity 48 (4) (2018) 812–830.e814, https://doi.org/10.1016/j.immuni.2018.03.023.
[56] M. Yang, M.J. Schell, A. Loboda, et al., Repurposing EGFR inhibitor utility in colorectal cancer in mutant APC and TP53 subpopulations, Cancer Epidemiol. Biomarkers Prev. 28 (7) (2019) 1141–1152, https://doi.org/10.1158/1055-9965.epi-18-1383.
[57] D. Maeser, R.F. Gruener, R.S. Huang, oncoPredict: an R package for predicting in vivo or cancer patient drug response and biomarkers from cell line screening data, Briefings Bioinf. 22 (6) (2021), https://doi.org/10.1093/bib/bbab260.
[58] P.W. Eide, J. Bruun, R.A. Lothe, A. Sveen, CMScaller: an R package for consensus molecular subtyping of colorectal cancer pre-clinical models, Sci. Rep. 7 (1) (2017), 16618, https://doi.org/10.1038/s41598-017-16747-x.
[59] X. Bao, Q. Li, J. Chen, et al., Molecular subgroups of intrahepatic cholangiocarcinoma discovered by single-cell RNA sequencing-assisted multiomics analysis, Canc. Immunol. Res. 10 (7) (2022) 811–828, https://doi.org/10.1158/2326-6066.Cir-21-1101.
[60] M. Shin, P. Petersen, S. Lau-Rivera, et al., Actionable fusions detected by RNA-seq co-occur with PD-L1 expression and driver mutations in solid tumors patients, 1254, Cancer Res. 82 (12_Supplement) (2022) 1254.